

Evaluation of the Adsorption Process Using Low Cost Agroindustry Residue for the Removal of Methylene Blue Dye

Fabiano Mendonça de Oliveira^{a*}, Priscila Afonso Rodrigues de Sousa^b, Edmar Isaías de Melo^a, and Luciana Melo Coelho^b

^aFederal University of Uberlândia, Institute of Chemistry, Monte Carmelo Campus, 38500-000, Monte Carmelo-MG, Brazil.

^bFederal University of Goiás, Special Academic Unit of Physics and Chemistry, 75704-020 Catalão-GO, Brazil.

Article history: Received: 22 July 2019; revised: 30 April 2020; accepted: 07 May 2020. Available online: 28 June 2020. DOI: <http://dx.doi.org/10.17807/orbital.v12i2.1422>

Abstract:

The activities of the textile industry consume a lot of water, generating a high volume of effluents, contributing to the increase of contaminant levels. Adsorption has been pointed out as a promising technique for the removal of effluent dyes. Agroindustry wastes are alternative materials of low cost, since considerable quantities of these are discarded in the environment and already have been reported the potential of these materials as adsorbents in the removal of pollutants. In this sense, the present work evaluated the use of the orange peel as adsorbent material in the removal of the methylene blue dye in aqueous medium by adsorption. The characterization of the residue was evaluated using scanning electron microscopy and infrared spectroscopy. The time required for the system to reach equilibrium was 40 min, following the kinetics described by the Pseudosecond Order Parameters. The maximum adsorptive capacity verified was 62.89 mg g⁻¹, following the Langmuir isotherm model, however the model that best fit was Freundlich, indicating adsorption in multilayers. In this way, the obtained results showed that the orange peel presents potential application as adsorbent in the treatment of organic pollutants in specific, cationic dyes present in liquid effluents.

Keywords: dye; low cost adsorbent; methylene blue; orange peel

1. Introduction

Nowadays the environmental issue has become one of the main focuses of world public interest, since the residues produced from the human activities already surpass the natural capacity of auto depuration of the biosphere, and they are accumulating in the air, in the waters and solos, or causing environmental degradation at a faster rate than natural regeneration. Inevitably the challenges of environmental issues permeate all activities related to industrial processes [1].

Among the wide range of industrial sectors in Brazil, the textile industry is known worldwide as one of the largest consumers of water in its production processes (80-100 m³ / ton of finished fabric) and, consequently, one of the largest generators of industrial effluents [2]. Water is used

for cleaning the raw material and for many washing steps throughout the production and the effluents formed are composed of a wide variety of chemicals and dyes, which makes them an environmental challenge [3].

It is estimated that about 10-15% of the textile dyes used are released into the effluent during the dyeing phase [4], and the presence of very low concentrations (less than 1 mg L⁻¹) in the effluent is visible and considered undesirable. The release of these effluents into natural environments is problematic for both aquatic life and human health due to their mutagenic effects. More than 90% of the 4,000 dyes tested by the Ecological and Toxicological Association of the Dyestuffs Manufacturing Industry (ETAD) showed toxicity, with the highest rates found among alkaline dyes [5].

*Corresponding author. E-mail: mendonca_fabiano@hotmail.com

Among the most applicable dyes is the class of reagents, among them methylene blue, a cationic dye, widely used in the textile industry in the dyeing of cotton and wool fabrics, generating effluent that affects not only the transparency of the water, but also limits the passage of solar radiation decreasing the natural photosynthetic activity causing changes in the aquatic biota, originating acute and chronic toxicity of aquatic ecosystems [6].

In view of the potential risk presented by these textile effluents to the environment, it is necessary to develop alternative and efficient treatment processes since conventional methods are economically unfavorable and / or technically complex. In this sense, adsorption appears as an alternative process for the removal and recovery of effluents using adsorbent materials, which present low cost, availability, high capacity and adsorption rate [7].

The adsorbents most used commercially are activated carbon, zeolite, silica gel and activated alumina, however, due to the high costs, alternative adsorbents have been studied in the treatment of industrial effluents, with emphasis on agroindustry residues [8].

Among these, the waste generated in the orange industries deserves to be highlighted, the accumulation of which results in the occupation of land and consequently in the pollution by phenolic compounds due to its improper disposal. Since the orange peel is available in the processing industries, recycling these residues for wastewater treatment not only has an economic advantage, but also contributes to minimizing problems with the disposal of this residue, which represents 50% of its gross weight [9]. The literature reports several studies using orange peel as an adsorbent material for the treatment of effluents contaminated by metals [10,11] and dyes [12,13,14].

The orange peel is largely composed of cellulose pectin, hemicellulose, lignin and other low molecular weight compounds, including limestone. It can be used as an efficient and low cost adsorbent for removing organic dyes from industrial effluent. In addition, orange peel is an alternative to adsorbent for its abundance in nature and for being biodegradable [14].

Based on the previously mentioned

assumptions, residues from the agroindustry, among them the orange peel and its application as adsorbent used to remove contaminants can be a promising alternative for the remediation of effluents by the adsorption process, given their availability, character of renewable product, requirement of little preparation and low cost for its use. Considering the characteristics and advantages of the orange peel, together with the advantages of the adsorption process for effluent remediation, the present work aimed to evaluate the orange peel as an alternative adsorbent material applied in the removal of the methylene blue dye in aqueous medium by adsorption.

2. Material and Methods

2.1. Preparation and characterization of the adsorbent

The orange residues were obtained from local commerce in Monte Carmelo-MG. The orange residue was cut into pieces, separating the husk from the bagasse; then the bark was crushed and washed with deionized water and dried in an oven with air circulation at 45 °C until constant mass. The granulometric separation of the barks was carried out in a sieve with a mesh of 0.25 mm. The characterization of the adsorbent material was performed by infrared spectrometry using a FTIR Prestige-21 Infrared Spectrophotometer, Shimadzu. The spectra were recorded from 4000 to 500 cm^{-1} . The surface morphology was evaluated using an JSM-6610 Scanning Electron Microscope.

2.2. Calibration curve for quantitative analysis of methylene blue dye

The cationic dye, methylene blue (C.I. 52030, $\text{C}_{16}\text{H}_{18}\text{N}_3\text{SCl}_4$) obtained from Sigma Chemical, USA, with analytical grade and was used without further purification. A stock solution at the concentration of 100 mg L^{-1} in deionized water was used for the preparation of standard solutions in different concentrations (0.1, 0.5, 1.0, 2.0, 4.0, 6.0; 8.0 and 10 mg L^{-1}) with pH adjusted to the value of 8.00 with pH meter, Hanna Instruments, model HI255, used to construct the calibration curve. The absorbance of the standard solutions was evaluated with Hach's UV-Vis spectrophotometer, Model DR4000 at wavelength

665 nm.

2.3. Adsorption tests

The adsorption tests were performed by adding 10.0 mg of adsorbent material (mean particle diameter less than 0.25 mm) in 20.0 mL of dye solution (6 mg L⁻¹) kept under stirring for 20 min at the temperature environment. After this period the biomass was separated by centrifugation for 5 minutes at 3000 rpm and the final concentration of the dye in solution was determined using a UV-VIS spectrophotometer (HACH DR / 4000) at 665 nm, with detection limit , 0.4 mg L⁻¹ and limit of quantification of 0.12 mg L⁻¹. The amount of adsorbent dye per mass of the adsorbent at equilibrium (adsorptive capacity q_e) was calculated using Equation 1.

$$q_e = \frac{(C_0 - C_e)V_L}{m_{ads}} \quad \text{Equation (1)}$$

q_e = amount of adsorbed dye given in mg adsorbate g⁻¹ adsorbent; C_0 e C_e are the initial liquid phase and equilibrium concentrations, respectively (mg L⁻¹); V_L = volume of solution (L) and m_{ads} is mass of adsorbent (g).

2.4. Study of H influence on adsorption

The effect of pH was investigated in methylene blue dye solutions at different pH levels (2, 4, 6, 7, 8, 10 and 12) by adsorption tests (10.0 mg adsorbent material and 20, 0 mL of blue methylene solution, 6.0 mg L⁻¹, stirring time 20 minutes). The initial pH value was adjusted with solutions of HCl (0.1 mol L⁻¹) and NaOH (0.1 mol L⁻¹) using pH meter, Model HI 2223-01, Hanna brand.

2.5. Adsorption kinetics

Adsorption tests using 10.0 mg of adsorbent material and 20.0 mL of methylene blue solution (6 mg L⁻¹) and initial pH of 8.00 were performed at different shaking times (5, 20, 40, 60 and 120 minutes). In order to evaluate the adsorption kinetic process, the parameters of Pseudofirst Order, Pseudosecond Order, Parameters Intraparticle diffusion and Chemisorption were applied.

2.6. Adsorption isotherms

Adsorption tests were carried out with 50.0 mL solution at different concentrations of methylene blue (6.0, 12.0, 18.0, 24.0, 28.0, 32.0, 36.0, 40.0, 44.0 and 48.0 mg L⁻¹), initial pH equal to 8. The stirring time and mass of the adsorbent material were 40 minutes and 20 mg, respectively. The values of C_e , amount of solute adsorbed in the fluid phase (mg L⁻¹) and q_e , amount of solute adsorbed in the solid phase (mg g⁻¹) were calculated and the Langmuir and Freundlich models were used to evaluate the equilibrium adsorption.

3. Results and Discussion

The adsorption phenomenon occurs due to the presence of functional groups that constitute the adsorbent material; the infrared was then used to identify these groups. The infrared spectrum for the orange peel, Figure 1, shows an intense band at 3416 cm⁻¹ which is attributed to the stretching vibrations of the bond (OH), belonging to the structure of cellulose and hemicellulose, which constitutes the main component of lignocellulosic materials [15].

The bands caused by stretches at approximately 2926 cm⁻¹, (C-H), and bands at 1329 cm⁻¹ are attributed to the vibrations of the -CH₂ group present in cellulose and hemicellulose [16]. The presence of the bands at 1516, 1449 and 1636 cm⁻¹ are attributed to stretches (C = C) of aromatic groups isolated from lignin [17]. The vibrations in the 1728 cm⁻¹ region correspond to the elongation of the carbonyl of aldehydes. The 1249 cm⁻¹ band is attributed to the vibrations (C-O) of esters, ethers, or phenol groups [18].

The bands located at 1158 cm⁻¹ are derived from the stretching of the C-O-C group of glycosidic linkages β(1→4). The band present in 1012 cm⁻¹ must originate from the stretching of C-O in cellulose, hemicellulose and lignin, or stretching of C-O-C in cellulose and hemicellulose [19].

In this way it is possible to observe that the main oxygen groups present in the shell of the orange are distributed in the form of esters, ethers, alcohols and phenols. These groups may be associated to the adsorption process by the adsorbent material.

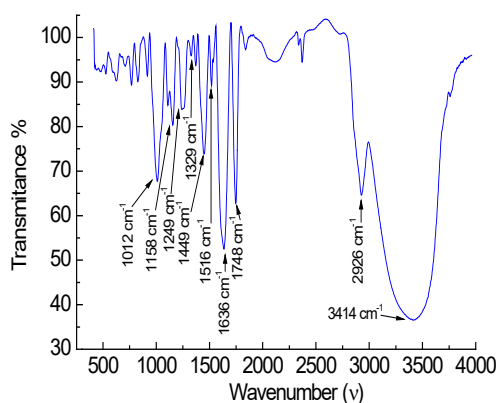


Figure 1. Infrared spectrum of the orange peel.

The surface of the adsorbent was also verified using scanning electron microscopy (SEM). The morphological characteristics of the orange peel surface (Figure 2) show irregularities, heterogeneous and quite complex morphology, with smooth and rough regions, behavior attributed to the drying process of dehydrated plant tissues [20,21].

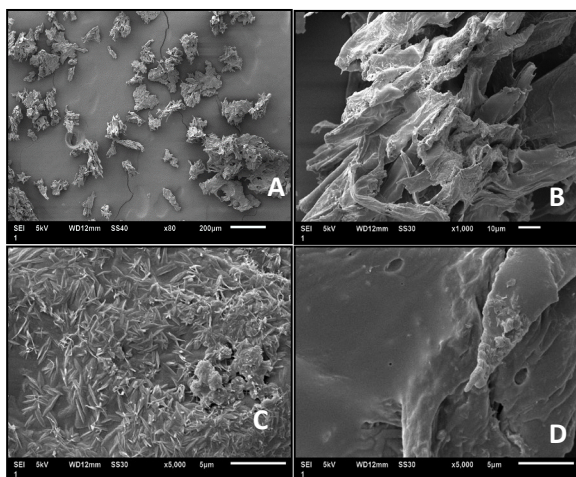


Figure 2. Scanning electron microscopy (SEM) micrographs of orange peel. Increase: 80X (A); 1000X (B); 5000X (C) and (D).

In addition, Figure 2B and 2C shows the heterogeneity of the particles, in shape and size, as well as high roughness. These characteristics are probably due to the mechanical action of grinding the adsorbent in its preparation, with consistent gradients and gradients [22].

Figure 2D and 2B, on the other hand, show smooth and rough regions, besides indicating the presence of few voids. This morphological characteristic can be an indication that the

material has low specific surface area [23]. It is possible to visualize that the adsorbent has a large contact surface area which may favor the removal of the methylene blue dye in aqueous medium.

Another factor influencing adsorption is the surface charge of the adsorbent in which the pH value of the solution indicates the ability of the surface to be charged positively or negatively. In this way, when the $\text{pH} < \text{pH}_{\text{PCZ}}$ the residue presents predominance of positive net surface charge being favored the adsorption of anions and in $\text{pH} > \text{pH}_{\text{PCZ}}$ the net surface charge will be negative favoring the adsorption of cations [24].

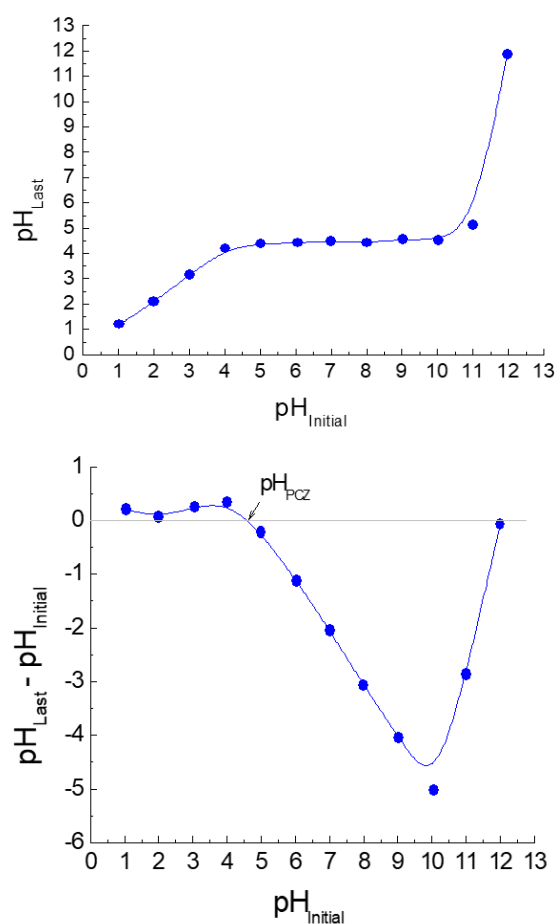


Figure 3. Zero load point of orange peel.

In alkaline media, the surface of the adsorbent material may present a negative net surface charge, as verified in the evaluation of the pH_{PCZ} (Figure 3), which favors the adsorption process of the cationic dye.

Methylene blue dye, depending on its concentration in the medium, may form aggregates, monomeric, dimeric and polymer

forms of this dye. In aqueous media the equilibrium of aggregate formation tends to be displaced in the sense of formation of ionic aggregates. Methylene blue's spectrum at 6 mg L^{-1} (Figure 4) show a maximum band of approximately 665 nm, corresponding to the monomer form of the dye, and a band around 610 nm, corresponding to a coupling transition characteristic of the dye [25].

Once the maximum absorption wavelength for the dye was determined, a standard analytical curve was obtained from reading the light absorption at $\lambda_{\text{max}} = 665 \text{ nm}$, standard methylene blue solutions at pH = 8.00, 1, 0.5, 1.0, 2.0, 4.0, 6.0, 8.0 and 10 mg L^{-1} (Figure 5).

The figures of merit of the method, sensitivity, limit of detection (LD), limit of quantification (LQ), linearity, working range are described in Table 1.

The detection limit (LD) is the smallest amount of analyte present in a sample that can be detected, under established experimental conditions. It is the minimum concentration of a measured and declared substance with 95 or 99% confidence that the analyte concentration is greater than zero [26]. Therefore, the detection limit can be considered as the smallest amount of analyte in a sample that can be detected but not necessarily quantified with an exact value [27]. The limit of detection was evaluated by the method based on parameters of the analytical curve according to the equation $\text{LD} = 3.0 \text{ } x_s / S$, where s is the estimate of the standard deviation of the target and S is the slope or angular coefficient of the analytical curve.

It is the lower limit of quantification (LQ) of a compound present in a sample that can be determined quantitatively with precision and accuracy [26,28]. For Swartz (2007), quantification limit is defined as the lowest concentration of an analyte in a sample that can be determined with acceptable accuracy and accuracy under the specific operating conditions of the method. The limit of quantification was evaluated by the method based on parameters of the analytical curve according to the equation $\text{LQ} = 10 \text{ } x_s / S$, where s is the estimate of the standard deviation of the blank and S is the slope or coefficient of the analytical curve.

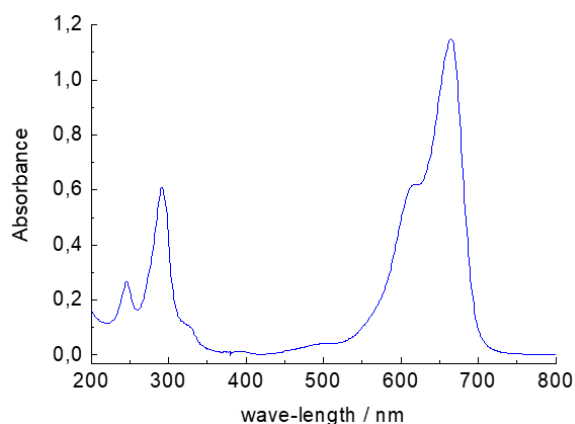


Figure 4. Absorption spectrum of aqueous methylene blue solution 6 mg L^{-1} .

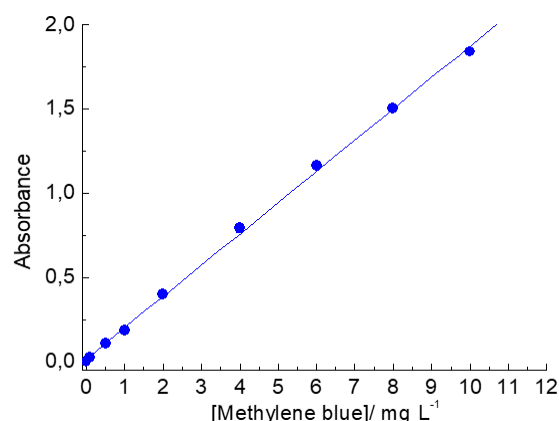


Figure 5. Calibration curve for methylene blue dye.

It is the lower limit of quantification (LQ) of a compound present in a sample that can be determined quantitatively with precision and accuracy [26,28]. For Swartz (2007), quantification limit is defined as the lowest concentration of an analyte in a sample that can be determined with acceptable accuracy and accuracy under the specific operating conditions of the method. The limit of quantification was evaluated by the method based on parameters of the analytical curve according to the equation $\text{LQ} = 10 \text{ } x_s / S$, where s is the estimate of the standard deviation of the blank and S is the slope or coefficient of the analytical curve.

According to INMETRO (2003), the working range is the concentration range of the analyte in which the method can be applied, that is, it is the interval between the lower and upper levels of analyte concentration in which it has been demonstrated the determination with accuracy, accuracy and linearity under the conditions specified in test. Linear working range can also be

defined range of analyte concentrations over which the method provides test results proportional to analyte concentration, or in which a linear model can be applied with a known confidence level [29].

Sensitivity is the ability of the method to distinguish, with a certain level of confidence, two contiguous concentrations. From the practical point of view, the sensitivity is the angular coefficient of the analytical chart [30,31].

Linearity is the ability of an analytical method to demonstrate that the results obtained are directly proportional to the analyte concentration in the sample within a specified range. It can be calculated from the linear regression equation, determined by the least squares [32].

Tests were performed by varying the initial pH of the solutions to verify the effect of this parameter on the adsorption of the dye, since the pH of the solution can modify the surface charge of the adsorbent, as well as influence the degree of ionization of the adsorbate molecule and on the degree of dissociation of functional groups on the active sites of the adsorbent [33]. The evaluation of the pH effect on the inorganic orange peel adsorption capacity is presented in Figure 6.

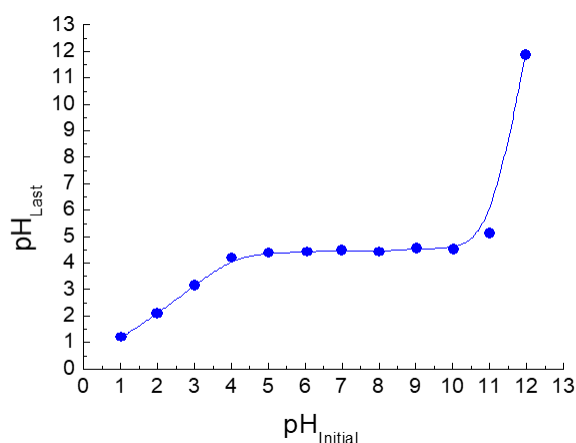


Figure 6. Adsorption capacity of the orange peel as function of the pH of the methylene blue solution.

The adsorptive capacity remains constant in a pH range between 7 and 12. The lowest values of adsorptive capacity were verified at pH 2. The adsorption increases with increasing pH, with the adsorption equilibrium being established from pH 7. The low adsorptive capacity in acid medium is probably due to the presence of excess H⁺ ions that compete with the cationic groups of the dye

and the adsorption sites. In alkaline media, the surface of the adsorbent material may present a negative net surface charge, as verified in the evaluation of the pH_{PCZ} (Figure 3), which favors the adsorption process of the cationic dye. The maximum adsorptive capacity, 73.82 mg g⁻¹, was verified at pH = 8.

The study of the adsorption kinetics is an important parameter used in studies related to the treatment of aqueous effluents, since it provides information about adsorption processes such as: the time required for each equilibrium, the adsorbate adsorption velocity [34].

Table 1. Figures of merit of the method.

Limit of detection-LD	0,04 mg L ⁻¹
Limit of quantification-LQ	0,12 mg L ⁻¹
Sensitivity	0,18587
Working range	0,1 a 10 mg L ⁻¹
Linearity	Abs = 0,01587 + 0,18587[C ₁₆ H ₁₈ N ₃ SCl]

Abs: Absorbance

The evolution of adsorption kinetics of the methylene blue dye to the solid phase, using as an adsorbent material the orange peel can be visualized in Figure 7.

Several kinetic models are used to examine the controlling mechanism of the adsorption process, such as chemical reaction, diffusion control and mass transfer. The most frequently used models are those of Pseudofirst Order and Pseudosecond Order [35]. However, the mechanism of the adsorption process cannot be obtained by these two models, requiring the application of other models, among them the Weber and Morris Intraparticle Diffusion model and the Elovich kinetic absorption model, for example.

The adsorption velocity can be determined by the expression of the Pseudofirst order velocity given by Lagergren for the adsorption in liquid / solid system based on the capacity of the solid. The adsorbate removal rate over time is directly proportional to the difference in saturation concentration and the number of active sites in the solid. The Lagergren kinetic equation is the most

used for the adsorption of an adsorbate of an aqueous solution [35].

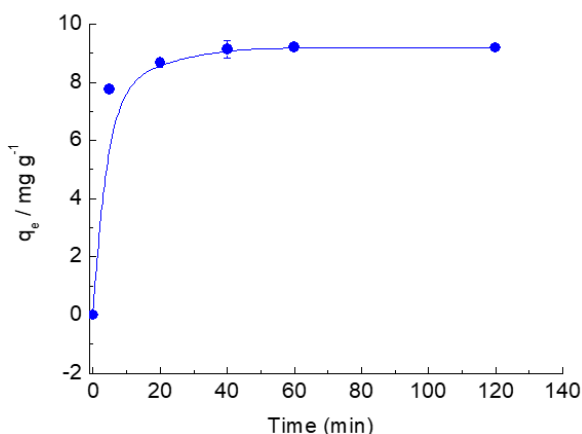


Figure 7. Effect of stirring time on the removal of the methylene blue dye for orange peel.

A simple analysis of the adsorption kinetics performed by the Pseudofirst order Lagergren equation based on the solids capacity is given by Equation 1 in its linearized form:

$$\frac{t}{q_t} = \frac{1}{k_2 q_e^2} + \frac{t}{q_e} \quad \text{Equation (2)}$$

The value of k_1 can be determined from the graph of $\ln(q_e - q_t)$ versus t . The adjustment of the equation to the experimental data requires that the adsorption capacity at equilibrium, q_e , be known [36].

The kinetic data were also analyzed using the Pseudosecond Order kinetics, where the reaction rate is dependent on the amount of solute adsorbed on the surface of the adsorbent and the adsorbed amount at equilibrium. The linear model of Pseudosecond Order can be expressed according to equation 3:

$$\frac{t}{q_t} = \frac{1}{k_2 q_e^2} + \frac{t}{q_e} \quad \text{Equation (3)}$$

The values of q_e and k_2 can be obtained through the intercept and slope of the curve shown in the graph (t/q_t) versus t . If the kinetic model of Pseudosecond Order is applicable, the plot of (t/q_t) versus t must have a linear relation close to 1 [36].

According to WEBER and MORRIS [37,38], if intraparticle diffusion is the speed determining factor, adsorbate removal varies with the square

root of time. Thus, the intraparticle diffusion coefficient (k_{dif}) can be defined by equation 4.

$$q_t = k_{dif} t^{1/2} + c \quad \text{Equation (4)}$$

being: q_t = the amount of adsorbed dye (mg g^{-1}); t = the stirring time (min); C (mg g^{-1}) = constant related to diffusion resistance.

The value of k_{dif} ($\text{mg g}^{-1} \text{min}^{-1/2}$) can be obtained from the slope and the C value of the intersection of the graph curve q_t versus $t^{1/2}$. The values of C give an idea of the thickness of the boundary layer, that is, the larger the value of C , the greater the effect of the boundary layer [36].

The Elovich equation is applied to the kinetics of chemisorption. This equation has been applied satisfactorily in some chemisorption processes and has been successfully applied in slow adsorption kinetics [38]. The kinetic equation is valid for systems in which the surface of the adsorbent is heterogeneous, equation 5.

$$q_t = \frac{1}{\alpha} \ln(\alpha \cdot \beta) + \frac{1}{\beta} \ln(t) \quad \text{Equation (5)}$$

Being: α = the initial rate of adsorption ($\text{mg g}^{-1} \text{min}^{-1}$); β = constant related to the degree of coverage and the activation energy involved in the chemisorption process (g mg^{-1}).

In order to evaluate adsorption kinetics, the experimental data described in figure 7 were adjusted to the models of Pseudofirst Order, Pseudosecond Order, Weber and Morris Intraparticle Diffusion and Elovich Chemisorption, and the kinetic parameters of the adjustment of these models presented in the Table 2.

In addition, the values of q_e calculated for this model, $9,244 \text{ mg g}^{-1}$ showed good agreement with the values of q_e obtained experimentally $9,186 \text{ mg g}^{-1}$. This model indicates that the reaction rate is dependent on the amount of solute adsorbed on the surface of the adsorbent and on the adsorbed amount in the equilibrium [41].

The adsorption behavior can be evaluated quantitatively through adsorption isotherms. They express the relationship between the amount of the dye that is adsorbed per unit mass of the adsorbent and the concentration of the dye in equilibrium solution at constant temperature. The

graphic expression of the isotherm is generally a hyperbole.

The adsorption can be evaluated quantitatively through the isotherms. The equilibrium study provides fundamental information to evaluate the ability of different adsorbents to adsorb a given adsorbate, in order to obtain an estimate of the maximum amount of contaminant to be adsorbed [42, 43].

Table 2. Kinetic parameters for the removal of methylene blue using orange peel. Experimental conditions: $m/v=0,5 \text{ mg L}^{-1}$; $\text{pH}=8$ e $C_0=6 \text{ mg L}^{-1}$.

Pseudofirst Order	$K_f(\text{min}^{-1})$	0.0201
	$q_e(\text{mg g}^{-1})$	1.6680
	R^2	0.3139
	F_{error}	1.3210
Pseudosecond Order	$K_s(\text{g mg}^{-1}\text{min}^{-1})$	0.1668
	$q_e(\text{mg g}^{-1})$	9.2438
	$h_0(\text{mg g}^{-1}\text{min}^{-1})$	14.257
	R^2	0,9999
	F_{error}	0.0568
Chemisorption	$\alpha(\text{mg g}^{-1}\text{min}^{-1})$	6.1564
	$\beta(\text{g mg}^{-1})$	0.5603
	R^2	0.8712
	F_{error}	1.9911
Intraparticle diffusion	$K_{\text{dif}}(\text{mg g}^{-1}\text{min}^{-1/2})$	0.6917
	C	3.6603
	R^2	0.7489
	F_{error}	2.6878

The shape of the isotherm plot is determined by the adsorption mechanism and can be used to suggest the type of adsorption that occurs between the adsorbent and the adsorbate. To define the isotherm profile is an important point in the studies related to the adsorption process, since they do not always have the same profile, and depend on the nature of the adsorbent, the adsorbate and the conditions of the medium, such as pH, temperature and others.

The classification given by Giles *et al.* [44] is based on the initial inclinations and curvatures of the isotherms. The high affinity (H), Langmuir (L), constant (C), and sigmoid (S) [45]. By observing the plateaus, inflection points and maximal, the isotherms can be classified into subgroups. This classification is based on observation and does

not reveal the connection between the process and the shape of the isotherm [46].

In general, S-type isotherms are concave at low concentrations. While the isotherms H and L are convex, the slope of the isotherms H reaches high values and the isotherms L are constant. This indicates that the sorption affinity of the H isotherms increases with the decrease in concentration. C-type isotherms are defined by the constant sorption affinity expressed by a straight line. The subgroups are defined by their behavior at high concentrations, subgroup 1 does not present plateaus, subgroup 2 is characterized by having 1 plateau, subgroup 3 has a point of inflection due to the change to concave shape. Two plateaus are characteristic of subgroup 4 [47].

According to the Giles classification the isotherm for the orange peel (Figure 8), it is of type S-1, which indicates that the adsorption increases as the number of adsorbed molecules increases (cooperative adsorption).

The Langmuir and Freundlich isotherms models are the most frequently used to describe the adsorption equilibrium, applied technique in water and effluent treatment [47].

The Langmuir isotherm is widely used in numerous adsorption processes mainly in the adsorption of dyes on solid surfaces. The Langmuir equation is an equilibrium isotherm based on a theoretical model which relates the amount of solute adsorbed on a surface to the concentration of the solute in the solution. This model is based on the hypothesis that the maximum adsorption occurs in a monolayer saturated with adsorbate molecules on the surface of the adsorbent that is energetically homogeneous containing a finite number of identical sites. The formation of the monolayer depends on the assumption that the intermolecular forces decrease with the distance and with this only a single layer of solute adsorbed must occur. The model assumes uniform sorption energies at the surface and there is no transmigration of the adsorbate in the surface plane. According to the Langmuir model, adsorption occurs at specific sites and is also available for adsorption [48].

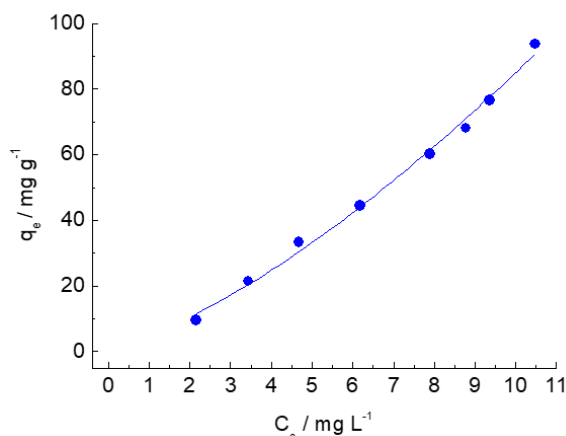


Figure 8. Orange peel adsorption isotherm.

All sites are equivalent, and the surface is uniform, a molecule attaches to a site independently of the others being occupied or not. In theory, the adsorbent has a finite capacity for the adsorbate [49]. The Langmuir isotherm is represented by equation 5.

$$\frac{C_{eq}}{q_e} = \frac{1}{k_L q_{max}} + \frac{C}{q_{max}} \quad \text{Equation (6)}$$

Considering C_e/q_e as dependent variable and C_{eq} as independent variable, we obtain the values of K_L and q_{max} , where $1/(K_L q_{max})$ is the linear coefficient and $1/q_{max}$ is the angular coefficient of the line. From the adsorption

parameters obtained, it is possible to evaluate the maximum adsorption capacity of the adsorbate by the adsorbent.

The Freundlich isotherm is an empirical adsorption isotherm for non-ideal adsorption on heterogeneous surfaces as well as for multilayer adsorption [49]. The Freundlich isotherm is given by equation 7:

$$\log q_e = \log k_F + \frac{1}{n} \log C_e \quad \text{Equation (7)}$$

Since: K_F = Freundlich constant characteristic of the system and indicative of adsorption capacity; n = Freundlich constant indicating the adsorption intensity; q_e = adsorbed amount (mg g^{-1}).

The values of K_F and n can be obtained by the intersection and slope of the linear graph of $\log q_e$ vs $\log C_e$. The value of n between 1 and 10 indicates favorable adsorption.

With the experimental results obtained, the parameters of the isotherms were calculated according to the Langmuir and Freundlich models, in order to verify if the experimental isotherm obtained follows the behavior of some of these, because although the empirical models do not reflect the questions related to the adsorption mechanism, they provide useful information on the adsorption capacity of an adsorbent [50].

The Langmuir model considers the surface monolayer sorption with a defined number of available places. The Freundlich model, on the other hand, considers that the sorption occurs in heterogeneous surfaces. The calculated parameters are shown in Table 3.

Table 3. Adsorption constants according to the Langmuir and Freundlich models for the removal of methylene blue using orange peel. Experimental conditions: $m/v = 400 \text{ mg L}^{-1}$, stirring time = 40 min, $\text{pH}=8$ and ambient temperature.

Langmuir	$q_{max} (\text{mg g}^{-1})$	62.890
	$K_L (\text{L mg}^{-1})$	0.0039
	R_L	0.9610
	R^2	0.8989
Freundlich	n	0.7905
	$1/n$	1.2650
	$K_F (\text{L mg}^{-1})$	4.5370
	R^2	0.9823

The values of the adsorption constants show that the Freundlich model fits very well to the experimental data obtained for the orange peel, as can be observed by the values of the correlation coefficients, R , presented (Table 3).

The value of q_{max} reflects high adsorptive capacity, possibly due to the greater availability of carboxyl groups present in the adsorbent material. Freundlich's n parameter is related to the intensity of the adsorbate interaction with the adsorbent, and n values in the range $1 < n < 10$ indicate favorable adsorption, which was observed for the adsorbent material. The value of the constant $n < 1$ indicated that the adsorption occurred by a cooperative process at sites with different binding energies. The constants K_F and $1/n$ are Freundlich constants. The K_F constant is an approximate measure of the adsorption capacity of the adsorbent. The higher the value, the greater the adsorption capacity. The values of R_L ($0 < R_L < 1$)

indicated that the adsorption process was favorable for the concentration range studied.

The orange peel presents cellulose, hemicellulose and lignin in its structure [51], which may favor adsorption, a fact that corroborates with the result obtained by the adsorption isotherm that demonstrates the efficiency of the orange peel as an adsorbent. The value of q_{\max} obtained by the Langmuir model reflects high adsorptive capacity for methylene blue in relation to other adsorbent materials reported in the literature, such as eucalyptus leachates of the *Eucalyptus grandis* species ($q_{\max} = 12.41 \text{ mg g}^{-1}$) [52], sugarcane bagasse ($q_{\max} = 31.79 \text{ mg g}^{-1}$) [53] and passion fruit bark ($q_{\max} = 44.70 \text{ mg g}^{-1}$) [54], the orange peel being 62.89 mg g^{-1} .

4. Conclusions

The results show that the orange peel presents potential application as adsorbent material in the remediation of specific organic pollutants, dyes in liquid effluents. The orange peel appears as an economically viable alternative to the commercial adsorbents, since these materials present a high cost pertinent to the production, especially activated carbon. Another relevant point of this material is its availability, easy processing, it is a renewable source and presented efficiency in the removal of the methylene blue dye. In the kinetic study it was verified that the equilibrium was reached in 40 min and the model that best fitted the experimental data was the Pseudosecond Order. The Freundlich model was the one that best adjusted, presenting a linear correlation value close to 1. The maximum adsorptive capacity verified was 62.89 mg g^{-1} .

References and Notes

- [1] Hang, G.; Liang, C. Z.; Chung, T. S.; Weber, M.; Staudt, C.; Maletzko, C. *Water Res.* **2016**, *91*, 361. [\[Crossref\]](#)
- [2] Savin, I. I.; Butnaru, R. *Environ. Eng. Manage. J.* **2008**, *7*, 859. [\[Link\]](#)
- [3] Oller, I.; Malato, S.; Sánchez-Pérez, J. A. *Sci. Total Environ.* **2011**, *409*, 4141. [\[Crossref\]](#)
- [4] Gita, S.; Hussan, A.; Choudheny, T. G. *Environ. Ecology* **2017**, *35*, 2349. [\[Link\]](#)
- [5] Robinson, T.; McMullan, G.; Marchant, R.; Nigam, P. *Bioresour. Technol.* **2001**, *77*, 247. [\[Crossref\]](#)
- [6] Kunz, A.; Peralta-Zamora, P.; Moraes, S. G.; Duran, N. *Quím. Nova.* **2002**, *25*, 78. [\[Link\]](#)
- [7] Loukidou, M. X.; Matis, K. A.; Zouboulis, A. I.; Kyriakidou, L. M. *Water Res.* **2003**, *37*, 4544. [\[Crossref\]](#)
- [8] Pollard, S. J. T.; Fowler, G. D.; Sollars, C. J.; Perry, R. *Sci. Total Environ.* **1992**, *116*, 3331. [\[Crossref\]](#)
- [9] El Nemr, A.; Abdelwahab, O.; El-Sikaily, A.; Khaled, A. *J. Hazard. Mater.* **2009**, *100*, 102. [\[Crossref\]](#)
- [10] Pérez Marín, A. B.; Ortuño, J.F.; Aguilar, M.I.; Meseguer, V.F.; Sáez, J.; Lloréns, M. *Biochem. Eng. J.* **2010**, *53*, 2. [\[Crossref\]](#)
- [11] Guo, X. Y.; Liang, S.; Tian, Q. H. *Adv. Mater. Res.* **2011**, *236–238*, 237. [\[Link\]](#)
- [12] Mafra, M. R.; Igarashi-Mafra, L.; Zuim, D. R.; Vasques, É. C.; Ferreira, M. A. *Rev. Bras. Eng. Quím.* **2013**, *30*, 657. [\[Crossref\]](#)
- [13] Zhul-quarnain, A.; Ogemdi, I. K.; Modupe, I.; Gold, E.; Chidubem, E. E. *J. Biomater.* **2018**, *2*, 31. [\[Link\]](#)
- [14] Abdurrahman, F. B.; Akter, M.; Abedin, M. *Inter. J. Scient. Tec. Research* **2013**, *2*, 47. [\[Link\]](#)
- [15] Yang, H.; Yan, R.; Chen, H.; Lee, D. H.; Zheng, C. *Fuel* **2007**, *86*, 1781. [\[CrossRef\]](#)
- [16] Cao, Y.; Tan, H. *J. Mol. Struct.* **2004**, *705*, 189. [\[Crossref\]](#)
- [17] Brown, C.; Antony, P.; Martin, A. P.; Grof, C. P. L. *J. Integr. Agric.* **2017**, *16*, 1256. [\[Crossref\]](#)
- [18] Hoareau, W.; Trindade, W. G.; Siegmund, B.; Castellán, A.; Frollini, E. *Polym. Degrad. Stab.* **2004**, *86*, 567. [\[Crossref\]](#)
- [19] Oh, S. Y.; Yoo, D. I.; Shin, Y.; Kim, H. C.; Kim, H. Y.; Chung, Y. S.; Park, W. H.; Youk, J. *Carbohydr. Res.* **2005**, *340*, 2376. [\[Crossref\]](#)
- [20] Agustí, M.; Almela, V.; Juan, M.; Alférez, F.; Tadeo, F. R.; Zacarías, L. *Ann. Bot.* **2001**, *88*, 415. [\[Crossref\]](#)
- [21] Fernandez, M. E.; Nunell, G. V.; Bonelli, P. R.; Cukierman, A. L. *Ind. Crops Prod.* **2014**, *62*, 437. [\[Crossref\]](#)
- [22] Piccin, J. S.; Gomes, C. S.; Feris, L. A.; Gutterres, M. *Chem. Eng. J.* **2012**, *183*, 30. [\[Crossref\]](#)
- [23] Wang, L.; Li, J. *Ind. Crops Prod.* **2013**, *42*, 153. [\[Crossref\]](#)
- [24] Özacar, M.; Sengil, I. A. *J. Hazard. Mater.* **2003**, *98*, 211-224, 2003. [\[Crossref\]](#)
- [25] Patil, K.; Pawar, R.; Talap, P. *Phys. Chem. Chem. Phys.* **2000**, *2*, 4313. [\[Crossref\]](#)
- [26] INMETRO-INSTITUTO NACIONAL DE METROLOGIA, NORMALIZAÇÃO E QUALIDADE INDUSTRIAL. Orientações sobre validação de métodos de ensaios químicos, DOQCGCRE-008, **2003**. [\[Link\]](#)
- [27] Swartz, M. E. *J. Liq. Chromatogr. Relat. Technol.* **2007**, *28*, 1253. [\[Crossref\]](#)
- [28] Rozet, E.; Marinia, R. D.; Ziemonsa, E.; Boulangerb, B.; Huberta, Ph. *J. Pharm. Biomed. Anal.* **2011**, *55*, 848. [\[Crossref\]](#)
- [29] Taveniers, I.; De Loose, M.; Bockstaele, E.V. *TrAC, Trends Anal. Chem.* **2004**, *23*, 535. [\[Crossref\]](#)
- [30] Amarante Jr., O. P. de.; Caldas, E. P.A.; Brito, N. M.; Santos, T. C. R. dos S.; Vale, M. L. B. F. *Caderno de Pesquisa* **2001**, *12*, 116. [\[Link\]](#)

- [31] Brito, N. M.; Amarante Jr, O. P. de; Polese, L.; Santos, T. C. R. dos.; Ribeiro, M. L. *Pesticidas: Revista Ecotoxicologia e Meio Ambiente* **2002**, *12*, 155. [\[Link\]](#)
- [32] Valderrama, P.; Braga, J. W. B.; Poppi, R. J. *Quim. Nova* **2009**, *32*, 1278. [\[Link\]](#)
- [33] Mall, I. D.; Srivastava, V. C.; Agarwal, N. K.; Mishra, I. M. *Chemosphere* **2005**, *61*, 492. [\[Crossref\]](#)
- [34] Dotto, G. L.; Pinto, L. A. A. *J. Hazard. Mater.* **2011**, *187*, 164. [\[Crossref\]](#)
- [35] Simonin, J. P. *Chem. Eng. J.* **2016**, *300*, 254. [\[Crossref\]](#)
- [36] Debrassi, A.; Largura, M. C. T.; Rodrigues, C. A. *Quim. Nova* **2011**, *34*, 764. [\[Crossref\]](#)
- [37] Weber, W. J.; Morris, J.C. *J. Sanit. Eng. Div., Am. Soc. Civ. Eng.* **1963**, *89*, 31. [\[Link\]](#)
- [38] Oliveira, F. M. de; Coelho, L. M.; Melo, E. I. de. *Rev. Mater.* **2018**, *23*, 1. [\[Crossref\]](#)
- [39] Jacques, R. A.; Lima, E. C.; Dias, S. L. P.; Mazzocato, A. C.; Pavan, F. A. *Sep. Purif. Technol.* **2007**, *57*, 193. [\[Crossref\]](#)
- [40] Cardoso, N. F.; Lima, E. C.; Pinto, I. S.; Amavisca, C. V.; Royer, B.; Pinto, R. B.; Alencar, W. S.; Pereira, S. F. P. *Int. J. Environ. Technol. Manage.* **2011**, *92*, 1237. [\[Crossref\]](#)
- [41] Calvete, T.; Lima, E. C.; Cardoso, N. F.; Vaghetti, J. C. P.; Dias, S. L. P.; Pavan, F. A. *Int. J. Environ. Technol. Manage.* **2010**, *91*, 1695. [\[Crossref\]](#)
- [42] Ho, Y. S.; Mckay, G. *Process Biochem. Int.* **1999**, *34*, 451. [\[Crossref\]](#)
- [43] Roostael, N.; Tezel, F. H. *Int. J. Environ. Technol. Manage.* **2004**, *70*, 157. [\[Crossref\]](#)
- [44] Giles, S. N.; Macewan, C. H.; Nakhwa, T.H. *J. Chem. Soc.* **1960**, *1*, 3973. [\[Crossref\]](#)
- [45] Hinz, C. Description of sorption data with isotherm equations, *Geoderma* **2001**, *99*, 225. [\[Crossref\]](#)
- [46] Fungaro, D. A.; Izidoro, J. C.; Bruno, M. *Eletica Quim.* **2009**, *34*, 45. [\[Crossref\]](#)
- [47] Walker, G. M.; Weatherley, L. R. *Chem. Eng. J.* **2001**, *83*, 201. [\[Crossref\]](#)
- [48] Özcan, A. S.; Özcan, A. *J. Colloid Interface Sci.* **2004**, *276*, 39. [\[Crossref\]](#)
- [49] Aksu, Z.; Tezer, S. *Process Biochem. Int.* **2005**, *40*, 347. [\[Crossref\]](#)
- [50] Do Duong, D. Adsorption Analysis: Equilibria and Kinetic, 3rd ed. London: Imperial College Press, 1998. [\[Crossref\]](#)
- [51] Cypriano, D. Z.; da Silva, L. L.; Mariño, M. A; Tasic, L. *Rev. Virtual Quim.* **2017**, *9*, 176. [\[Crossref\]](#)
- [52] De Marchi, H. F.; Soeiro, T. N.; Halasz, M. R. T. *Anais do XI Congresso Brasileiro de Engenharia Química em Iniciação Científica* **2015**, *1*, 1. [\[Link\]](#)
- [53] Silva, W. L. L. D.; Oliveira, S. P. D. *Sci. Plena* **2012**, *8*, 1. [\[Link\]](#)
- [54] Pavan, F. A.; Dias, S. L. P.; Mazzocato, A. C. *J. Hazard. Mater.* **2008**, *150*, 703. [\[Crossref\]](#)